

Spectral properties of systems with dynamical localization: I. The local spectrum

T Dittrich† and U Smilansky

Department of Nuclear Physics, The Weizmann Institute of Science, Rehovot 76100, Israel

Received 2 February 1990, in final form 15 October 1990

Accepted by M V Berry

Abstract. We study the correlations in the quasi-energy (QE) spectra of systems with dynamical localization, using the quantum kicked rotor (QKR) as a paradigm. The specific spatial structure of the QE eigenstates is taken into account by investigating the *local spectrum*, which gives each eigenstate an individual weight according to its overlap with some reference state. Two-point correlations in the local spectrum are related by Fourier transform to the time evolution of the probability to stay at the initial state. We devise a scaling theory for this dynamical quantity in the case of the QKR, containing the participation ratio as a single parameter. It implies that the local spectrum is characterized by *positive* correlations, in contrast to the unbiased spectra in classically chaotic systems with a bounded phase space. This is consistent with recent results on spectral properties of systems with Anderson localization. A scheme for experimental measurements of spectral two-point correlation functions is proposed.

PACS numbers: 0530, 0545, 7155J

1. Introduction

The search for the fingerprints of classical chaos in quantum systems has proceeded, in the last decade, mainly in two different directions. The study of time-independent systems with a bounded phase space has been concentrated on spectral features. It was shown that, as soon as the corresponding classical dynamics becomes chaotic, the spectral fluctuations, in the limit $\hbar \rightarrow 0$, obey universal distribution laws, as predicted by random matrix theory (RMT) [1]. Recently, this quantum-classical correspondence has been extended to the domain of chaotic scattering, where the fluctuations in the *S*-matrix eigenphases were shown to follow the statistics of Dyson's circular orthogonal ensemble (COE) [2].

On the other hand, results obtained for periodically driven systems, represented by the quantum kicked rotor (QKR) as a prototype, stress the fundamental difference between classical and quantal dynamics. Unbounded diffusion, as a hallmark of deterministic chaos in the classical versions of such systems, is suppressed in the quantal case by a dynamical interference effect akin to Anderson localization [3, 4]. This effect is intimately related to the nature of the quasi-energy (QE) spectrum and the corresponding eigenstates of the (unitary) one-cycle propagator (*Floquet operator*).

† Permanent address: Institut für Physik, Universität Augsburg, Memminger Straße 6, D-8900 Augsburg, Federal Republic of Germany.

The suppression of classical diffusion is due to the fact that the Floquet eigenstates are exponentially localized when expressed in the basis of the unperturbed rotor. Localization, as a feature of the eigenfunctions, is associated with a discrete eigenvalue spectrum. Spectral discreteness in systems with *dynamical localization* thus arises in a fundamentally different way, compared with systems where the accessible phase space is restricted by boundary conditions. It is to be expected that this difference in the underlying dynamics is reflected in the statistical properties of the spectrum.

A straightforward application of the results obtained for Dyson's circular ensembles [5, 6] is certainly not justified in this case: a basic property of the canonical ensembles is the invariance of their statistical properties under rotations, such that any basis can be chosen equally well for their representation. Localization, on the other hand, introduces a highly specific, representation-dependent structure of the eigenstates. In particular, it implies that eigenstates localized at sufficiently separated sites become effectively uncorrelated [7]. As a consequence, the nearest-neighbour distribution is rendered Poissonian, despite the chaotic nature of the corresponding classical dynamics [7–9]. This situation has no analogue in the theory of the canonical ensembles; it should be taken into account by incorporating spatial structures into the spectral statistics.

In the present paper, we pursue this idea by analysing in detail a specific example, the QE spectrum of the QKR. The question of how spectral statistics are influenced by localization has a longer history in the quantum theory of disordered media than in quantum chaology. Therefore, it is natural to adopt concepts and methods of spectral analysis which have proven useful in the context of Anderson localization. The fact that randomness in the QKR is based on an underlying *deterministic* dynamics, on the other hand, can be exploited by using the powerful semiclassical techniques developed in the quantum chaology of time-independent and scattering systems.

Specifically, we investigate two-point correlation functions for two different types of QE spectra, both of which are sensitive to spatial structures, and are inspired by analogous concepts in solid state theory: the *local spectrum* and the *unbiased spectrum for a finite sample*. Two-point correlations allow to derive the Δ_3 statistics [1] and form an essential building block for the derivation of the traditional nearest-neighbour (NN) distribution. Beyond that, they also contain information on the large QE scales, and they appear in the expressions for observables, thus providing a direct link to dynamical properties. Our main result is that these correlation functions, in the case of the QKR, bear the marks of classical deterministic diffusion as well as of quantum localization. Dynamical localization is reflected in novel features of the spectral fluctuations, different from those derived for any one of Dyson's circular ensembles.

The local spectrum is obtained by assigning to each QE value a weight, equal to the probability for the corresponding eigenstate to overlap with a local site, specified as an eigenstate of the unperturbed Hamiltonian [3]. This procedure involves fractional weights which depend in a complicated way on the positions of the eigenstates. Therefore the local spectrum cannot be generated by selecting eigenstates 'by hand' from the full QE basis, upon diagonalization of the Floquet operator. It is, however, intimately connected to a dynamical quantity which provides direct analytical and experimental access: correlations in the local spectrum are related by Fourier transform to the time evolution of the population of the state in which the system was prepared initially. This function, called the *staying probability*, contains essential information on the dynamics. In systems with localization, it decays diffusively during the initial stages of the evolution and approaches asymptotically the inverse of the number of accessed states. Conversely, characteristic dynamical features translate into properties

of the local spectrum: a relationship well known, e.g., in quantum chemistry [10]. We utilize it to demonstrate that dynamical localization is reflected in the local spectrum by a tendency to display *level clustering* at small QE separations. As a matter of fact, a similar result has recently been obtained in the context of Anderson localization [11–13]. There, level clustering could be explained by the occurrence, at avoided level crossings, of QE eigenstates with two (or more) centres of localization, a mechanism initially proposed by Mott [14]. The apparent attraction is thus revealed to be solely due to a strong increase, with decreasing QE separation, of the relative weight given to pairs of QEs in the local two-point correlation function. This is sufficient to overcompensate the repulsion of the bare levels. We suggest a corresponding interpretation for the case under study, thereby adding a new aspect to the analogy between quantum chaos and the quantum mechanics of random media.

The analogue of a finite sample is introduced, in the context of dynamical localization, by restricting the infinite-dimensional Hilbert space spanned by the unperturbed Hamiltonian to a finite-dimensional subspace. The time evolution in the truncated space of dimension L remains unitary and approaches the evolution of the unrestricted QKR for $L \rightarrow \infty$. The L quasi-energies of the truncated system can be treated on equal an footing by assigning the same weight to all of them. This approach will be investigated in a forthcoming publication [15]; it will serve, in particular, to study systematically the dependence of the spectral statistics on the parameter γ , defined as the ratio of the mean localization length in the unmodified system to the finite basis size.

In order to set the stage for the discussion of spectral properties we introduce, in a preparatory section 2, notations and basic partly novel concepts to be used in the description of the classical and quantal dynamics of the kicked rotor. In particular, we propose a simple one-parameter scaling theory for the time evolution of the staying probability. Section 3 is devoted to the study of the local spectrum. Its relation to the staying probability is used to translate the scaling *ansatz* developed in section 2 into the functional form of the two-point correlations characterizing the local spectrum. A scheme of how to measure spectral correlation functions experimentally, providing a possible test of our theory, is proposed in section 4. We summarize our results in section 5.

Before going into the subject itself, we give a brief account of important results obtained by other investigators in the field.

Feingold *et al* [7] were among the first to investigate the influence of localization on the QE statistics. They studied biased ensembles of quasi-energies of the QKR which were obtained by selecting the associated eigenfunctions according to the separation of their approximate centres of localization. As long as states within the same localization neighbourhood are sampled, the nearest-neighbour distribution of QE levels resembles the Wigner–Dyson ensemble appropriate to classically chaotic systems with the symmetry properties of the kicked rotor. If, on the other hand, the sampled states are separated by more than a typical localization length, the spectrum displays a Poissonian distribution characteristic of the superposition of several mutually uncorrelated spectra. Their result reflects the gradual switching off, with increasing separation, of communication between the eigenstates involved. The dependence of the spectral statistics on the effective Planck's constant, as a complementary question, has been investigated by Frahm and Mikeska [16] (see also the comment of Feingold *et al* on this work, and the reply by Frahm and Mikeska [17]). The Poissonian behaviour of the nearest-neighbour distribution for the unrestricted spectrum was also noted by

Izrailev [9].

Blümel *et al* [18] studied the statistics of the QE spectrum for the hydrogen atom in a periodic external field. They selected the QE states according to their overlap with the classical chaotic domains in phase space, and showed that if the overlap is large, level repulsion dominates the spectrum, whereas if it is small, the NN distribution is Poissonian.

Izrailev [9] took another approach by restricting the dynamics to a finite basis, in such a way that the unitarity of the Floquet operator is preserved. Resembling our finite sample approach introduced above, the ratio γ of localization length to basis size forms an important parameter in this case also. In particular, the spectral fluctuations show a transition from Wigner–Dyson type for $\gamma \gg 1$, to Poissonian for $\gamma \rightarrow 0$, similar to the transition mentioned above in the context of biased ensembles. Recently, Izrailev [19] was able to fit the nearest-neighbour distribution functions for all values of γ by a simple expression which appears like an extension of the Wigner formula. So far, however, this approach is still phenomenological.

2. Classical diffusion and quantum localization

The present study makes use of the kicked rotor [20] as a paradigm of the class of periodically driven systems with one freedom which displays chaotic features in their classical dynamics. Since we intend to use classical quantities in semiclassical and quantum expressions in the sequel, it is convenient to measure angular momenta and actions in units of \hbar from the beginning. In such a notation, the Hamiltonian describing the kicked rotor is given by

$$H(l, \theta) = \frac{l^2}{2} + k \cos(\theta) \sum_n \delta(t - n\tau) \quad (2.1)$$

with a cylindrical classical phase space $-\infty < l < \infty$, $0 \leq \theta < 2\pi$.

The kicked rotor possesses two basic symmetries which we state for further reference: It is invariant against time reversal (denoted by T), corresponding to the operation

$$l \rightarrow -l \quad \theta \rightarrow \theta \quad t \rightarrow -t. \quad (2.2)$$

A less common, purely geometric symmetry is the invariance of the Hamiltonian (2.1) against reflections with respect to the origin of phase space (denoted by P),

$$l \rightarrow -l \quad \theta \rightarrow 2\pi - \theta. \quad (2.3)$$

We shall refer to the combination of these two symmetries (denoted by C, $C = PT$),

$$l \rightarrow l \quad \theta \rightarrow 2\pi - \theta \quad t \rightarrow -t \quad (2.4)$$

as ‘conjugation’.

A version of the standard map corresponding to the Hamiltonian (2.1) is obtained by integrating the equations of motion between $t_n = n\tau + \epsilon$ and $t_{n+1} = (n+1)\tau + \epsilon$, $\epsilon \rightarrow 0^+$,

$$\begin{aligned} l_{n+1} &= l_n + k \sin(\theta_{n+1}) \\ \theta_{n+1} &= (\theta_n + \tau l_n) \bmod 2\pi. \end{aligned} \quad (2.5)$$

In addition to the symmetries (2.2)–(2.4) of the Hamiltonian, this map is periodic not only in θ but also in the angular momentum l , with period $2\pi/\tau$.

The dynamics generated by the classical standard map becomes globally chaotic if the classical stochasticity parameter $K = k\tau$ exceeds the threshold $K_c \approx 1$. A basic approximation of the time evolution in this regime, providing a simple picture of the long-time dynamics, is its description as a diffusion process: an ensemble of classical trajectories, prepared initially at $l = l_0$ and spread homogeneously in θ , will, at a time n , be distributed in angular momentum according to [21]

$$P_{cl}(l_0 \rightarrow l; n) = \frac{1}{\sqrt{2\pi Dn}} \exp\left(-\frac{(l-l_0)^2}{2Dn}\right) \quad (2.6)$$

where $D \approx k^2/2$ is the diffusion constant. This description, however, becomes valid only from the time n_d on, given by the timescale on which correlations in the classical dynamics decay. It can roughly be estimated as the inverse of the mean Lyapunov exponent associated with the classical map.

The quantum map, obtained from (2.1) by canonical quantization [21], is defined by the Floquet operator

$$U = \exp\left(-ik \cos(\hat{\theta})\right) \exp\left(-\frac{1}{2}i\tau \hat{l}^2\right). \quad (2.7)$$

The angular momentum and angle operators \hat{l} , $\hat{\theta}$, respectively, obey the commutation relation $[\hat{l}, \hat{\theta}] = -i$. Eigenstates and eigenvalues of the angular momentum operator are given by $|\hat{l} l\rangle = |l\rangle$, $l = 0, \pm 1, \pm 2, \dots$; they are collectively referred to as the unperturbed basis throughout this work. The Floquet eigenvectors and the corresponding QE will be denoted by $|\alpha\rangle$ and ω_α , respectively. Both families of eigenstates span the infinite Hilbert space which is the quantum analogue of the classical cylindrical phase space.

The localization of the Floquet eigenvectors is intimately connected with the measure of the corresponding QE spectrum. If the spectrum is point-like, the Floquet states are localized. Otherwise they are delocalized, i.e. they are not normalizable. There exists a rigorous criterion to distinguish between these two situations: consider the function

$$P_s(n) = \left\langle \left| \sum_{\alpha} e^{i\omega_\alpha n} |\langle \alpha | l \rangle|^2 \right|^2 \right\rangle \quad (2.8)$$

which corresponds classically to the mean probability to return to an initial condition specified with respect to angular momentum l , but independent of θ . The angle brackets indicate averaging over a sufficiently large number of initial states $|l\rangle$, e.g., over a subset of the unperturbed basis covering many localization neighbourhoods. The symbol \int indicates that both discrete and continuous components of the QE spectrum are included, if they exist. It has been proven that the quantity

$$\xi^{-1} = \lim_{N \rightarrow \infty} \frac{1}{N} \sum_{n=0}^{N-1} P_s(n) \quad (2.9)$$

indicates whether the eigenstates are localized and hence determines the character of the QE spectrum—if ξ^{-1} vanishes, the spectrum is continuous, whereas if ξ^{-1} is finite,

the spectrum contains a point-like component [22]. The fact that $\xi^{-1} \neq 0$ implies normalizability at least of a subset of the Floquet eigenstates, but does not indicate any particular form of their localization.

This theorem allows for a simple physical interpretation [10]: the function $P_s(n)$ gives the average population left at a time n , in an initial state prepared as an angular momentum eigenstate $|l\rangle$. This probability can vanish asymptotically for long times only if the eigenstates of the Floquet operator cover the entire space, i.e. if they are delocalized. In case they are localized, $P_s(n)$ must remain finite on average, and provides an estimate of the number of QE states overlapping appreciably with the initial state. Indeed, by substituting (2.8) in (2.9), we get

$$\xi^{-1} = \left\langle \sum_{\alpha} |\langle \alpha | l \rangle|^4 \right\rangle. \quad (2.10)$$

This is the definition of the mean *inverse participation ratio*. For systems with exponential localization, the participation ratio ξ is proportional (with a proportionality factor of the order of 1) to the localization length.

The QKR does not show localization for values of the parameter τ/π that are either rationals [23] or Liouville numbers (irrational numbers for which the continued fraction approximation converges exceptionally fast) [24–26], both classes forming subsets of measure zero of the real numbers. There is ample numerical evidence (but no rigorous proof) in support of the observation that the QKR does localize for all other values of τ/π . We shall restrict the discussion from now on to the latter, generic case, where the Floquet eigenstates are normalizable and the staying probability approaches a non-zero constant.

The function $P_s(n)$, and in particular its transient behaviour is of special interest here. It allows us to formulate a scaling theory for the saturation of classical diffusion by quantum localization in the QKR system. Following the basic analysis of this crossover proposed in [27], we distinguish an initial phase of the time evolution, where the quantal dynamics essentially mimic the classical, and an asymptotic phase, dominated by the effects of localization.

The diffusion approximation for the classical dynamics (see (2.8)) predicts an algebraic decay of the probability to return to l_0 ,

$$P_s^{\text{cl}}(n) \approx \frac{1}{\sqrt{2\pi n D}} \quad n > n_d \gtrsim 1. \quad (2.11)$$

It gives the correct time dependence also for the initial decay of the staying probability in the quantal case. However, it does not take a basic quantum coherence effect into account which enhances the quantal staying probability by a factor of two, compared with the classical case: in a system symmetric with respect to conjugation, (2.4), there exist ‘conjugate pairs’ of trajectories closed in angular momentum. These are pairs of trajectories which return, after N time steps, to their respective initial values of l (but are not necessarily periodic), and are related by the transformation

$$l'_{n-1} = l_{N-n} \quad \theta'_n = 2\pi - \theta_{N-n} \quad (2.12)$$

so that $l'_0 = l_{N-1}$. For a conjugate pair of trajectories, semiclassical amplitudes are identical so that they contribute coherently to the probability to stay, (2.11). Thus

the staying probability is increased by an effective factor of two, except for the trivial case $n = 1$ (i.e. $N = 1$ in (2.12)) where closed trajectories coincide with their conjugate counterparts. Therefore, an approximation for the quantal staying probability in the initial phase, analogous to (2.11), is given by

$$P_s(n) \approx \sqrt{2/\pi n D} \quad \text{for small } n, \text{ but } n > n_d. \quad (2.13)$$

In the regime of large n , on the other hand, the discreteness assumed for the QE spectrum implies (see (2.9)) that

$$P_s(n) \rightarrow \xi^{-1} \quad \text{for } n \rightarrow \infty. \quad (2.14)$$

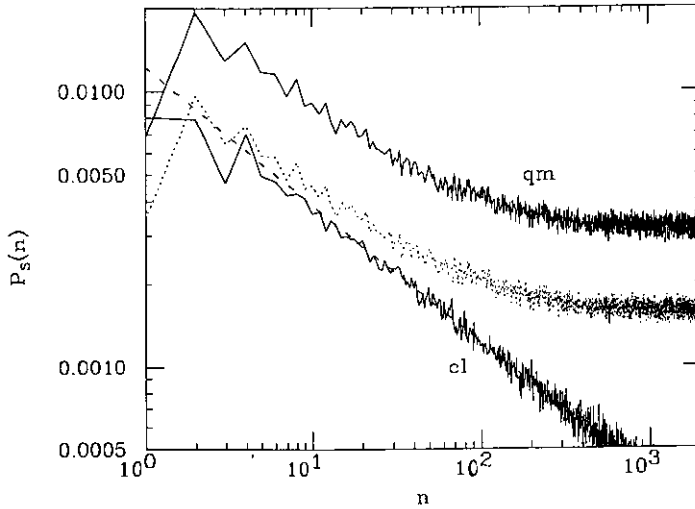


Figure 1. Evolution, over the first 2^{10} time steps, of the staying probability for the quantum mechanical (qm) and classical (cl) versions of the kicked rotor. Parameter values are $K = 20$, and $\tau = 0.05/((\sqrt{5} - 1)/2)$ in the quantum mechanical case, so that $k = K/\tau = 39.3$. The dotted graph represents the quantum mechanical function, reduced by a factor of two, which corresponds to the enhancement by constructive interference of paths with their conjugate counterparts, see (2.12). The broken line indicates the asymptotic decay $\propto 1/\sqrt{n}$ of the staying probability in the classical case.

In figure 1 we compare the time evolution of the staying probability $P_s(n)$ for the classical and the quantum mechanical versions of the kicked rotor (the classical data are based on an ensemble average over 5×10^5 trajectories, the quantum mechanical function was obtained by averaging incoherently over 512 'runs' of the QKR with equidistant initial states $|l\rangle$, separated by several localization lengths between neighbours). The classical stochasticity parameter was chosen $K = 20$, well above the critical value for the onset of global chaos, and the effective Planck's constant is $\tau = 0.05/g$ ($g = (\sqrt{5} - 1)/2$ denotes the golden mean), so that $k = K/\tau = 39.35$.

In the classical case, after a non-generic initial phase extending over several time steps, the staying probability decays according to the algebraic law (2.11), indicated by the broken line. The corresponding quantum mechanical function approaches the classical one as an asymptote for short times, if the quantum mechanical enhancement,

in systems with C invariance, of the probability to return is taken into account (the dotted graph represents the quantum mechanical data, reduced by the corresponding factor of two).

We introduce a scaling ansatz by assuming that the function $P_s(n)$ for all $n > n_d$ depends on the two parameters k and τ of the Floquet operator (2.7) only via a single scaling parameter, namely ξ . The two asymptotic forms (2.13) and (2.14) are reconciled if $\xi \sim D$ and, for $n > n_d$,

$$P_s(n) = \frac{1}{\xi} f(n/\xi) \quad (2.15)$$

where $f(x)$ is a scaling function which satisfies

$$f(x) \approx \begin{cases} \sqrt{2c/\pi x} & x \leq 1 \\ 1 & x > 1. \end{cases} \quad (2.16)$$

c is a constant to be determined from numerical data.

We have checked the validity of the scaling ansatz (2.16) numerically. Representative data are presented in figures 2 and 3. Figure 2(a) shows the scaling function $f(x) = \xi P_s(n)$, $x = n/\xi$, for the QKR at three different values of the effective Planck's constant, $\tau = 0.05/g$ (full line), $0.1/g$ (broken line), and $0.2/g$ (dotted line), while $K = 20$, as in figure 1. The corresponding values of the participation ratio, used for the rescaling, have been obtained from the mean long-time asymptotes of the staying probability as $\xi = 314, 90, 20$, respectively. It is clearly visible that all three curves, within the range of the fluctuations, describe the same functional dependence. In figure 2(b) we compare three different cases which differ in the classical kicking strength, keeping τ constant. Again, the three functions collapse to a single line upon rescaling. These results confirm the validity of our scaling ansatz (2.16).

Additional information about the scaling function is obtained by plotting $f(x) - 1$ (figure 3). This function emphasizes the way the staying probability approaches a constant for $n \rightarrow \infty$. It shows that this approach can be described by $f(x) - 1 \sim 1/x$ for $x \gtrsim 1$.

The scaling theory implies the well known relation between the classical diffusion constant D and the participation ratio ξ which, in turn, is proportional to the localization length. In the present notation, it reads

$$\xi = cD. \quad (2.17)$$

Our numerical data yield the estimate $c = 0.3 \pm 0.05$. The proportionality of ξ and D , (2.17), is demonstrated by the inset in figure 4, which is based on the same three sets of data as figure 2(a). The histogram shown in figure 4 represents the distribution of the 512 individual values of the inverse participation ratio ξ^{-1} , gathered in the case $\tau = 0.05/g$, $K = 20$. This distribution exhibits a single, pronounced maximum, confirming that the mean inverse participation ratio is a statistically meaningful quantity.

The constant c determines the cross-over time n_{qm} at which the asymptote $f(x) = 1$ is reached. We observe that $f(x) - 1 \approx 0.1$ at $x \approx 1$ (see figure 3), which implies $n_{\text{qm}} \approx \xi$. This result is consistent with the known proportionality [27] obtained for the time evolution of the energy gain. In fact, the timescale n_{qm} has a very general significance—it gives the time beyond which interference effects dominate the dynamics of the QKR (see below).

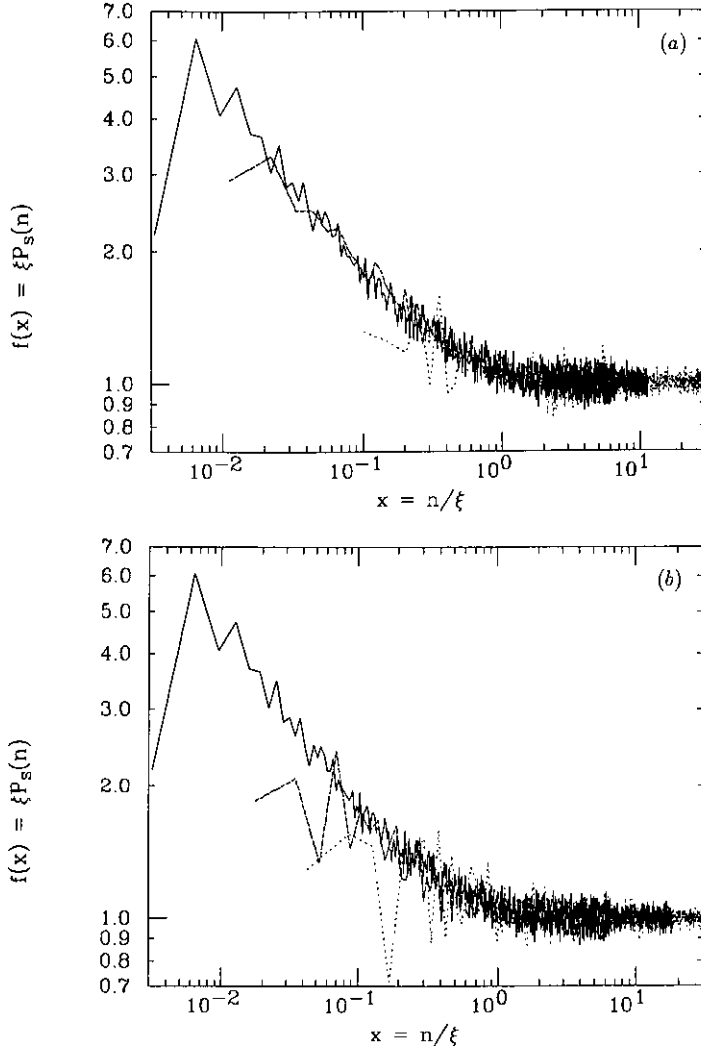


Figure 2. Scaled staying probability $\xi P_s(n)$ as a function of the scaled time $x = n/\xi$ for the quantum kicked rotor at three different values of the effective Planck's constant (a), and at three different values of the classical stochasticity parameter (b). Parameter values are (a) $K = 20$, and $\tau = 0.05/g$ (full line), $0.1/g$ (broken line), $0.2/g$ (dotted line); (b) $\tau = 0.05/g$, and $K = 20$ (full line), 10 (broken line), 5 (dotted line), where $g = (\sqrt{5} - 1)/2$. The corresponding values of the quantal parameter $k = K/\tau$ are $k = 39.3$ (full line), 19.7 (broken line), 9.8 (dotted line), for both parts.

Summarizing, we state as a crude estimate of the time evolution of the staying probability,

$$P_s(n) \approx \begin{cases} 1 & n = 0 \\ \sqrt{2c/\pi n \xi} & 1 \lesssim n_d < n \leq \xi \\ 1/\xi & n > \xi. \end{cases} \quad (2.18)$$

It becomes exact in the semiclassical limit, which amounts here to $\xi \rightarrow \infty$. Equation (2.18) is not valid for very short times, due to our neglect of the non-generic first kicks.

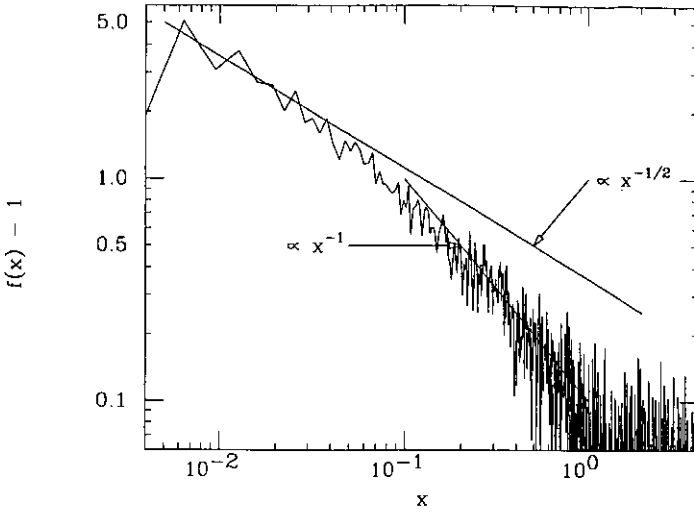


Figure 3. Scaled staying probability $\xi P_s(n) - 1$ as a function of the scaled time $x = n/\xi$ for the quantum kicked rotor. Parameter values are $K = 20$ and $\tau = 0.05/((\sqrt{5} - 1)/2)$. The left and right straight lines indicate algebraic decay as $x^{-1/2}$ and as x^{-1} , respectively.

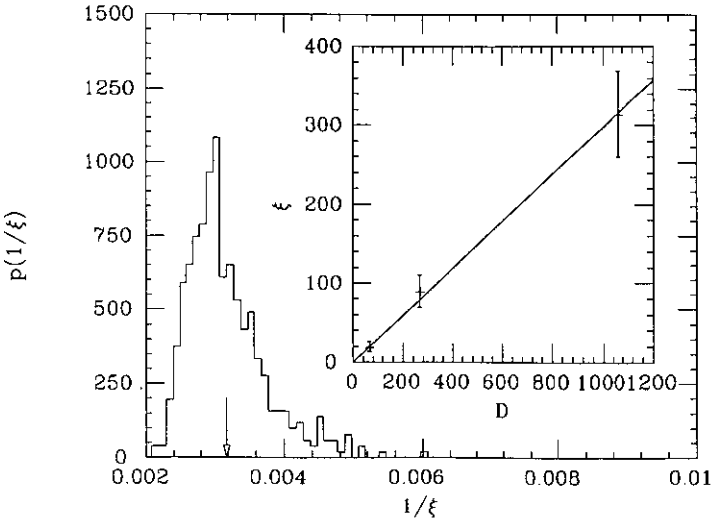


Figure 4. Probability distribution of individual values of the inverse participation ratio ξ^{-1} . Parameter values are $K = 20$ and $\tau = 0.05/((\sqrt{5} - 1)/2)$. The histogram is based on the long-time asymptotes of the staying probability for 512 different initial conditions. The arrow indicates the mean. Inset: mean values and RMS deviations of the measured participation ratios ξ , as a function of the diffusion constant D , for the three cases shown in figure 2(a).

It also fails to reproduce the cross-over from diffusion to quasi-periodicity as a smooth transition.

The above scaling theory, which combines both strictly classical and genuine quantum mechanical behaviour in a single expression, is most naturally studied from a semiclassical point of view. The staying probability is expressed semiclassically, as a

sum over paths, by

$$P_s(n) = \left\langle \left| \sum_r \sqrt{p_r(l;n)} \exp(i\Phi_r) \right|^2 \right\rangle. \quad (2.19)$$

The index r runs over the various classical orbits which start at and return to l after n time steps, $p_r(l;n)$ is the classical probability associated with the r th trajectory, and Φ_r is the corresponding action (the Maslov index is assumed to be absorbed in Φ_r). A reordering of the double summation over r , implied by (2.19), yields the alternative form

$$P_s(n) = \left\langle 2 \sum_r p_r(l;n) \right\rangle + \left\langle \sum_{r \neq r'} \sqrt{p_r(l;n)p_{r'}(l;n)} \exp(i(\Phi_r - \Phi_{r'})) \right\rangle. \quad (2.20)$$

The first term represents, besides a factor of two, the classical staying probability which decays as $1/\sqrt{n}$. Hence the second term includes genuine quantum coherence effects and should provide a semiclassical expression determining the inverse localization length. Conjugate pairs of trajectories are excluded from this term. As long as $n \lesssim n_{\text{qm}}$, however, its contribution is marginal and diffusive behaviour prevails. This behaviour is entirely due to the chaotic dynamics of the classical kicked rotor. For short times n , closed classical trajectories are scarce, the differences $\Phi_r - \Phi_{r'}$ between various action integrals are large, and, upon averaging, the non-diagonal elements in (2.20) cancel. The situation changes as soon as $n \gtrsim n_{\text{qm}}$: due to the exponential proliferation of closed trajectories with n and the fact that $\langle \Phi_r \rangle \sim n^2$, action differences $\Phi_r - \Phi_{r'}$ become sufficiently small to reach the order of unity, and therefore interference terms cease to average out. A direct evaluation of the inverse participation ratio from the non-diagonal term of (2.20) is beyond our present understanding of the semiclassical approximation. Yet, its genuine quantum mechanical origin is clear.

With these remarks we have completed the preparation of background and tools necessary to discuss spectral two-point correlation functions in the following section.

3. The local quasi-energy spectrum

In their work on the analogy between dynamical localization in the QKR and Anderson localization, Fishman *et al* [3] adopted a concept well known in the theory of electronic states in disordered solids to introduce the *local spectrum* for periodically driven systems. Its density is defined by

$$P_1(l; \omega) = \sum_{\alpha} |\langle \alpha | l \rangle|^2 \delta(\omega - \omega_{\alpha}). \quad (3.1)$$

(Here and in the following, delta functions of quasi-energies are understood to be 2π periodic.) The definition (3.1) assigns a weight $|\langle \alpha | l \rangle|^2$ (where $0 \leq |\langle \alpha | l \rangle|^2 \leq 1$) to each QE ω_{α} . The summation in (3.1) comprises the entire Floquet basis, so that the local density is normalized to unity.

By resolving the periodic delta functions in (3.1) into a Fourier sum, and using the defining property of the states $|\alpha\rangle$ to be eigenstates of the Floquet operator U , the local spectrum can alternatively be defined as

$$P_1(l; \omega) = \frac{1}{2\pi} \sum_{n=-\infty}^{\infty} e^{-i\omega n} A(l; n) \quad (3.2)$$

where

$$A(l; n) = \langle l | U^n | l \rangle \quad (3.3)$$

denotes the *amplitude* to be in the initial state $|l\rangle$ after n cycles of the driving force.

Similarly, a two-point density can be defined by

$$P_2(l, m; \omega, \chi) = \sum_{\alpha \neq \beta} |\langle \alpha | l \rangle|^2 |\langle \beta | m \rangle|^2 \delta(\omega - \omega_\alpha) \delta(\chi - \omega_\beta). \quad (3.4)$$

Here, each pair of QE values $\omega_\alpha, \omega_\beta$ is weighted by the product of overlaps of the corresponding eigenstates $|\alpha\rangle, |\beta\rangle$ with two reference states $|l\rangle, |m\rangle$, respectively, in the unperturbed basis. Due to the exclusion of diagonal elements $\alpha = \beta$ from the summation in (3.4), P_2 is not normalized to unity. Rather,

$$\int_0^{2\pi} d\omega \int_0^{2\pi} d\chi P_2(l, m; \omega, \chi) = 1 - \gamma_{l,m} \quad (3.5)$$

where we introduced the abbreviation

$$\gamma_{l,m} = \sum_{\alpha} |\langle \alpha | l \rangle|^2 |\langle \alpha | m \rangle|^2. \quad (3.6)$$

This quantity measures the extent to which the two states $|l\rangle, |m\rangle$ can communicate through their overlap with any Floquet eigenstate $|\alpha\rangle$. More precisely, it is the time average of the probability to make the transition $l \rightarrow m$. Particularly, for $l = m$, it reduces to the inverse participation ratio ξ^{-1} introduced in the preceding section.

Systems like the QKR are statistically homogeneous along the unperturbed basis, i.e. besides fluctuations, the properties of the Floquet eigenstates do not depend on their position in that basis. Therefore, relevant information is extracted from quantities like the complete two-point distribution function defined in (3.4) by averaging over the mean position of the pair $|l\rangle, |m\rangle$ of reference states, retaining only their relative distance $\Lambda = l - m$ as a spatial argument,

$$P_2(\Lambda; \omega, \chi) = \left\langle \sum_{\alpha \neq \beta} |\langle \alpha | l \rangle|^2 |\langle \beta | l + \Lambda \rangle|^2 \delta(\omega - \omega_\alpha) \delta(\chi - \omega_\beta) \right\rangle. \quad (3.7)$$

Angle brackets denote averaging over a sufficiently large ensemble of unperturbed eigenstates $|l\rangle$.

Likewise, the statistical homogeneity of the QE spectrum around the unit circle suggests to average over the mean position of QE pairs. For quantities defined cyclically, the concepts of midpoint and relative distance are ambiguous. We base our definition on the *shorter* arc connecting two QEs ω and χ (rather than the counterclockwise one). This amounts to a 'retiling' of the (ω, χ) plane according to the rule: if the separation $|\omega - \chi|$ exceeds the value π , shift the larger one of the two QEs by 2π (see figure 5). If we then define

$$\Omega = \frac{1}{2}(\omega + \chi) \quad \eta = (\omega - \chi + \pi) \bmod 2\pi - \pi \quad (3.8)$$

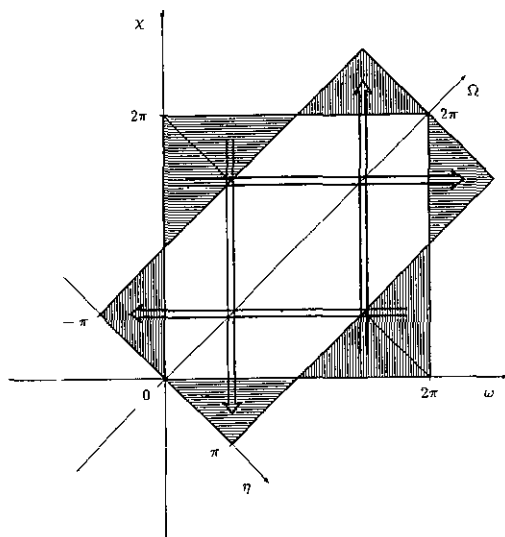


Figure 5. Transformation from quasi-energies ω, χ to their mean value Ω and relative separation η . The unit cell $0 \leq \omega, \chi < 2\pi$ transforms into the unit cell $0 \leq \Omega < 2\pi, -\pi \leq \eta < \pi$, if the hatched areas are shifted by an angle 2π with respect either to ω or to χ . This operation amounts to using the shorter arc connecting ω with χ as the basis of the transformation.

the (Ω, η) unit cell is obtained as the square $0 \leq \Omega < 2\pi, -\pi \leq \eta < \pi$.

The average over mean positions is now given by

$$P_2(\Lambda; \eta) = \int_0^{2\pi} d\Omega P_2(\Lambda; (\Omega + \eta/2) \bmod 2\pi, (\Omega - \eta/2) \bmod 2\pi). \quad (3.9)$$

This function may be interpreted as the joint probability to find two QE eigenstates with their centres of localization Λ quanta of angular momentum apart and, simultaneously, with their quasi-energies separated by an angle η .

The two-point correlation function (3.9) can also be written as a Fourier transform of a dynamical quantity. Here it is the correlator of the amplitudes to return from $|l\rangle$ to $|l\rangle$ and to return from $|l + \Lambda\rangle$ to $|l + \Lambda\rangle$, after n kicks,

$$P_2(\Lambda; \eta) = \frac{1}{2\pi} \sum_{n=-\infty}^{\infty} e^{-i\eta n} (\langle A(l; n) A^*(l + \Lambda; n) \rangle - \gamma_\Lambda) \quad (3.10)$$

where

$$\gamma_\Lambda = \langle \gamma_{l, l+\Lambda} \rangle. \quad (3.11)$$

Note that

$$\gamma_\Lambda = \lim_{N \rightarrow \infty} \frac{1}{N} \sum_{n=0}^{N-1} \langle A(l; n) A^*(l + \Lambda; n) \rangle \quad (3.12)$$

which ensures regular behaviour of $P_2(\Lambda; \eta)$ at $\eta = 0$.

We shall discuss the correlation function $P_2(\Lambda; \eta)$ separately for the two cases $\Lambda = 0$ and $\Lambda \neq 0$.

3.1. The case $\Lambda = 0$

The special case $\Lambda = 0$ of the relation (3.10) is of particular interest. It will henceforth be referred to as the *local two-point correlation function*, given by

$$P_2^{\text{loc}}(\eta) = \frac{1}{2\pi} \sum_{n=-\infty}^{\infty} e^{-i\eta n} (P_s(n) - \gamma_0). \quad (3.13)$$

Here, $P_s(n)$ is the mean *probability* to stay at a site $|l\rangle$ after n kicks, and $\gamma_0 = \xi^{-1}$ is the mean inverse participation ratio. Both quantities were defined and discussed above, where it was shown that ξ^{-1} is the asymptotic value of $P_s(n)$ for $n \rightarrow \infty$. We find therefore that the staying probability $P_s(n)$ is the Fourier transform of the local two-point correlation function P_2^{loc} .

Equations (3.10), (3.13) are the basic analytical tools used in the subsequent arguments, since they relate *spectral* correlations to products of *dynamical* staying amplitudes. The function P_2^{loc} has a close relative in RMT: multiplying it by the factor ξ^2 defines the function

$$R_2^{\text{loc}}(\eta) = \xi^2 P_2^{\text{loc}}(\eta) \quad (3.14)$$

which can be considered as the local analogue of the pair distribution function $R_2(\eta)$ [5, 6], introduced in RMT as the probability for any two eigenphases to be separated by an angle η , integrated over the positions of all other eigenphases. Accordingly, R_2^{loc} is normalized to the effective number of non-identical QE pairs,

$$\int_0^{2\pi} d\eta R_2^{\text{loc}}(\eta) = \xi(\xi - 1). \quad (3.15)$$

In the statistical analysis of spectra it is customary to define the *cluster function* $Y_2(r)$ [1, 6]. It is the difference between the pair distribution function for an uncorrelated spectrum and the actual pair distribution. The argument r corresponds to the difference η measured in units of the mean spacing $2\pi/\xi$. It is important to note that whenever $Y_2(r)$ vanishes the spectrum does not possess pair correlations. If $Y_2(r)$ is *negative*, the pairs with this value of r have a *higher* probability than in an uncorrelated spectrum, while if it is *positive*, the corresponding probability is *lower*. Since in the present case the effective number of QE values is ξ , we get

$$\begin{aligned} Y_2^{\text{loc}}(r) &= \frac{1}{\xi} \left(1 - 2 \sum_{n=1}^{\infty} (\xi P_s(n) - 1) \cos \left(\frac{2\pi}{\xi} rn \right) \right) \\ &= 1 - 2\pi P_2^{\text{loc}} \left(\frac{2\pi}{\xi} r \right). \end{aligned} \quad (3.16)$$

The fact that $\xi P_s(n) - 1 \sim n^{-1}$ for $x \gg 1$ (see figure 3) ensures convergence of the Fourier sum in the definition of $Y_2^{\text{loc}}(r)$. As was shown in section 2, the function $\xi P_s(n)$ can be written in the form $f(n/\xi)$, where $f(x)$ is independent of the parameters of the QKR (see (2.15), (2.18) and figure 2). Hence, in the limit of large ξ , $Y_2^{\text{loc}}(r)$ also approaches a function which no longer depends on ξ . Using numerical data for the staying probability, we can calculate Y_2^{loc} for a typical case of the QKR (see figure 6). The most striking feature is, that $Y_2^{\text{loc}}(r)$ is *negative* at small distances (it must become

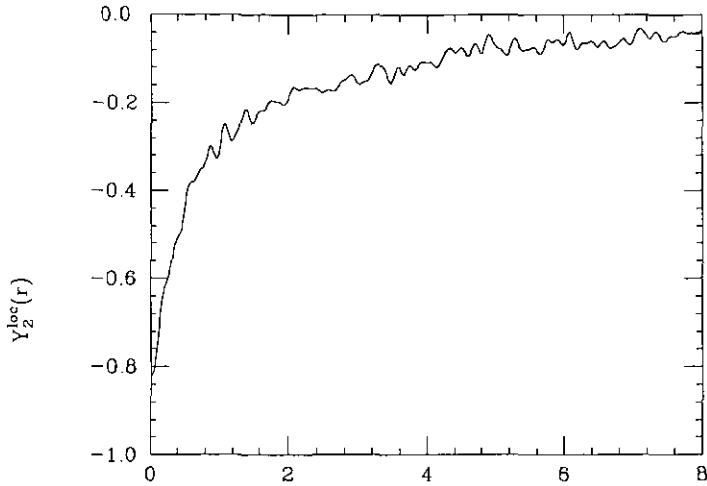


Figure 6. Local cluster function for the quantum kicked rotor. Parameter values are $K = 20$ and $\tau = 0.05/((\sqrt{5} - 1)/2)$. The function shown has been obtained by Fourier transform, according to (3.16), of the average quantal time evolution of the staying probability depicted in figure 1.

positive for large arguments, however, to ensure proper normalization). This implies that the *weighted* QE values tend to *cluster* at short distances.

This is a surprising result. It appears to be incompatible with the known, intuitive picture how dynamical localization gradually takes over in the time evolution of the QKR [27]: according to this view, as time n increases, the dynamics is influenced by ever finer QE scales $\Delta\omega$, given by the energy–time uncertainty relation $n\Delta\omega \gtrsim 2\pi$. As soon as the scale of the mean NN separation in the spectrum is reached, the dynamics crosses over from diffusive behaviour to quasi-periodicity. Arguing in the same spirit, we show in the sequel that the clustering of QEs in the local spectrum is not at variance with this picture, but refines it in essential points.

To begin with, it is important to note that the preparation of a very narrow initial state, compared even with the localized QE states, is a necessary condition for diffusion to occur in the first place; there is essentially no spreading of the wave packet if the system has been prepared in a state as wide as a typical QE state. In order to understand how a narrow state can arise by superposing eigenstates which decay only on a much larger scale, finer details of their structure have to be taken into account. The superposition of those eigenstates to form a narrow state is enabled only by the typical, erratic fluctuations around their *smooth exponential envelope*. Diffusive spreading can then be interpreted as a gradual destruction of the initial constellation of relative phases of the participating QE states with evolving time. They will mutually run out of phase due to the factors $\exp(i(\omega_\alpha - \omega_\beta)n)$ which generate the dynamics in the QE representation. Two states cease to contribute in a constructive way to the sharp initial state as soon as their accumulated relative phase $n(\omega_\alpha - \omega_\beta)$ has changed by an amount of the order of π . This process, in turn, is determined by the distribution of QE differences $\Delta\omega = \omega_\alpha - \omega_\beta$, *weighted* by the relative contribution of the associated pair of QE states $|\alpha\rangle, |\beta\rangle$ to the initial state. Thus it depends on the *local* two-point level correlation P_2^{loc} . As soon as the finest QE scale is reached, the quantum state no longer spreads on average, but merely fluctuates quasi-periodically around the superposition

of the exponentially decaying envelopes of the participating Floquet states. Since the effective fraction of Floquet states no longer contributing constructively to the initial state is roughly given by $\int_{\pi/n}^{\infty} d\eta P_2^{\text{loc}}(\eta)$, our result for the functional form of $P_2^{\text{loc}}(\eta)$ proves consistent with the intuitive view of the cross-over process and the corresponding estimate of its characteristic timescale.

Dealing with a closed system, we cannot actually call the process sketched here a 'loss of coherence'. In any specific instance of the dynamics, there are infinitely many recurrences, of any given accuracy, to the initial state. However, as soon as the corresponding classical dynamics becomes chaotic, these recurrences occur in a quasi-periodic pattern which is uniquely specific to the parameter values and the initial state chosen. Accordingly, they wash out in an appropriate *incoherent* average over a small neighbourhood of parameter values, or over a large ensemble of initial states, as we perform it here.

The arguments put forward in the preceding paragraphs leave an essential question open. In classically chaotic systems, instances of level separations far below the average are associated with *avoided crossings*, and the probability for avoided crossings to occur approaches zero as their width decreases. It can safely be assumed that this is the case for the QKR as well. A physical mechanism which explains how this same phenomenon, which gives rise to level *repulsion* in unbiased spectra, leads to an apparent *attraction* of levels in the local spectrum, has recently been proposed in the context of spectral features associated with Anderson localization [11–13]. It goes back to an idea originally proposed by Mott [14].

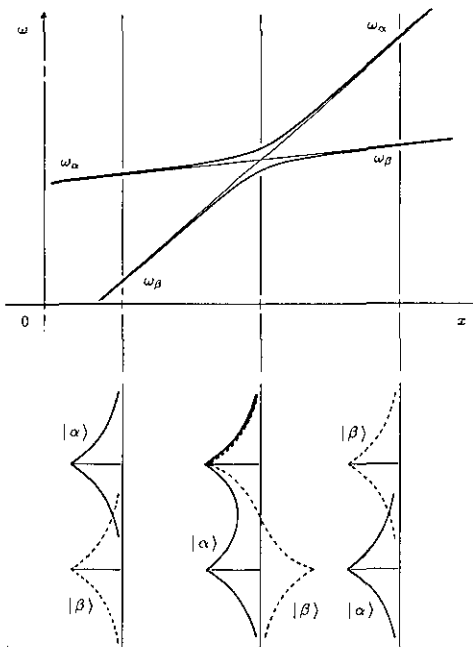


Figure 7. Schematic representation, for a system with dynamical localization, of two quasi-energies ω_α , ω_β and the corresponding eigenstates $|\alpha\rangle$, $|\beta\rangle$, as functions of a parameter x , in the neighbourhood of an avoided crossing. The exchange of identity of the two eigenstates proceeds, by a continuous turn of a mixing angle, through an intermediate stage where $|\alpha\rangle$ and $|\beta\rangle$ form symmetric and antisymmetric 'double-hump states', respectively.

Assume two localized QE states $|a\rangle$, $|b\rangle$ associated with a pair of QE levels ω_α , ω_β somewhat below an avoided crossing (see figure 7(a)), and follow the association of states with levels through the crossing: the eigenstates will remain associated with the eigenvalues in such a way as if the levels did cross without interaction, i.e. their association is gradually interchanged according to the turn of a mixing angle from 0 to $\pi/2$. Correspondingly, at the crossing point, they in fact consist of the symmetric and antisymmetric superpositions $|\alpha\rangle = (|a\rangle + |b\rangle)/\sqrt{2}$ and $|\beta\rangle = (|a\rangle - |b\rangle)/\sqrt{2}$, respectively, of the original states $|a\rangle$, $|b\rangle$ (see figure 7(b)). The states $|\alpha\rangle$ and $|\beta\rangle$, though still orthogonal to one another, will contribute to the local two-point correlation function with an exceedingly high weight, because this function is based on the overlap of probabilities and not of amplitudes. This suffices to overcompensate the decrease of unbiased probability for small separations.

Dynamically, this mechanism is associated with Rabi oscillations on an extremely slow timescale $2\pi/|\omega_\alpha - \omega_\beta|$, between $|a\rangle$ and $|b\rangle$; it is effective not only at the precise parameter value where the separation is minimal, but also in its neighbourhood. Its existence can be verified by demonstrating that there are 'double-hump states' among the QE eigenstates. Such states have indeed been observed at level crossings in systems related to the QKR [28]. Of course, simultaneous crossings of three or more levels are also feasible, albeit with even smaller probability. They would correspond to triple...-hump eigenstates and accordingly enhance the tendency towards level clustering in the local spectrum.

We can summarize our arguments by stating that the study of the local QE spectrum suggests a new feature of the quantum dynamics of classically chaotic periodically driven systems. The local QE correlations prefer clustering rather than repulsion of QE pairs. This phenomenon is closely connected to the suppression of classical diffusion by Anderson-like localization, and it is most clearly reflected in the probability to stay in the initial state. This latter function displays an interesting scaling property which emphasizes the intimate relation between the quantum localization length and the classical diffusion constant.

Our analysis also shows that among the various parameters which can be used to give a quantitative measure of localization, the inverse participation ratio seems to emerge as the natural choice. It stems out of the dynamical analysis of the staying probability and does not rely on an assumption concerning a particular functional dependence (e.g. exponential decay) of the wavefunction. It is distributed rather sharply about its mean (see figure 4), and thus is a useful tool in practice.

3.2. The case $\Lambda \neq 0$

In order to further illustrate the local spectrum approach, we give a brief account of the generalization to finite Λ of the correlation function (3.9),

$$\begin{aligned} P_2(\Lambda; \eta) &= \left\langle \sum_{\alpha \neq \beta} |\langle \alpha | l \rangle|^2 |\langle \beta | l + \Lambda \rangle|^2 \int_0^{2\pi} d\Omega \delta(\Omega + \eta/2 - \omega_\alpha) \delta(\Omega - \eta/2 - \omega_\beta) \right\rangle \\ &= \frac{1}{2\pi} \sum_{n=-\infty}^{\infty} e^{-i\eta n} (B(\Lambda; n) - \gamma_\Lambda) \end{aligned} \quad (3.17)$$

with

$$\gamma_\Lambda = \lim_{N \rightarrow \infty} \frac{1}{N} \sum_{n=0}^{N-1} B(\Lambda; n). \quad (3.18)$$

By analogy with (3.16), we define the *space-dependent cluster function* $Y_2(\Lambda; r)$ by

$$\begin{aligned} Y_2(\Lambda; r) &= 1 - 2\pi P_2\left(\Lambda; \frac{2\pi}{\xi} r\right) \\ &= \gamma_\Lambda \left(1 - 2 \sum_{n=1}^{\infty} (\gamma_\Lambda^{-1} B(\Lambda; n) - 1) \cos\left(\frac{2\pi}{\xi} rn\right)\right). \end{aligned} \quad (3.19)$$

The dynamical quantity $B(\Lambda; n)$, to which $P_2(\Lambda; \eta)$ is related by Fourier transform, is given by the product of two amplitudes,

$$\begin{aligned} B(\Lambda; n) &= \langle A(l; n) A^*(l + \Lambda; n) \rangle \\ &= \sum_{\alpha, \beta} e^{in(\omega_\alpha - \omega_\beta)} \langle |\alpha | l \rangle |^2 | \langle \beta | l + \Lambda \rangle |^2 \rangle. \end{aligned} \quad (3.20)$$

It has to be distinguished from the average probability of transitions over a distance Λ in the unperturbed basis, given by

$$\begin{aligned} P_t(\Lambda; n) &= \langle | \langle l + \Lambda | U^n | l \rangle |^2 \rangle \\ &= \sum_{\alpha, \beta} e^{in(\omega_\alpha - \omega_\beta)} \langle | l | \beta \rangle \langle \beta | l + \Lambda \rangle \langle l + \Lambda | \alpha \rangle \langle \alpha | l \rangle \rangle. \end{aligned} \quad (3.21)$$

Both quantities coincide only in their long-time averages,

$$\lim_{N \rightarrow \infty} \frac{1}{N} \sum_{n=0}^{N-1} B(\Lambda; n) = \gamma_\Lambda = \lim_{N \rightarrow \infty} \frac{1}{N} \sum_{n=0}^{N-1} P_t(\Lambda; n). \quad (3.22)$$

In contrast to the transition probability $P_t(\Lambda; n)$, a non-vanishing function $B(\Lambda; n)$ can arise only by genuine quantum interference effects and has no classical counterpart. We shall substantiate this statement, for the case of the QKR, by three arguments: a semiclassical analysis of $B(\Lambda; n)$, a quantum mechanical calculation of $B(\Lambda; n)$ for the first few time steps, and a numerical study.

By writing the amplitude $A(l; n)$ as a sum over paths,

$$A(l; n) = \sum_r \sqrt{p_r(l; n)} \exp(i\Phi_r) \quad (3.23)$$

and correspondingly for $A(l + \Lambda; n)$. Substituting it in (3.20), we obtain a semiclassical expression for $B(\Lambda; n)$, analogous to (2.19),

$$B(\Lambda; n) = \left\langle \sum_{r, r'} \sqrt{p_r(l; n) p_{r'}(l + \Lambda; n)} \exp(i(\Phi_r - \Phi_{r'})) \right\rangle. \quad (3.24)$$

Here, paths labelled r lead from l back to l , while paths r' lead from $l + \Lambda$ back to $l + \Lambda$. For $\Lambda = 0$, the staying probability is retained and the arguments given in section 2 apply exactly. For $\Lambda > 0$, diagonal elements in the proper sense no longer exist, since paths r are always different from paths r' (if Λ is not an integer multiple of the classical angular momentum period $2\pi/\tau$). However, for not too large Λ , this concept

can be generalized somewhat: by continuity, a difference Λ , small in classical units, between the initial conditions of two paths r, r' will lead only to a slight deformation of one path, compared to the other. This discrepancy may be neglected, to lowest order, in the probabilities p_r , but not in the phases, which, in the semiclassical limit, become increasingly sensitive even to classically small action differences. Thus, as a generalization for small Λ of the first term on the right-hand side in (2.20), we get the expression

$$B(\Lambda; n) \approx \left\langle 2 \sum_r p_r(l; n) \exp(i\Lambda \Delta\varphi_r) \right\rangle. \quad (3.25)$$

The factor two is due to the coherent contributions of conjugate pairs of trajectories (see (2.12)). We replaced the action difference $\Delta\Phi$ by the lowest term of its Taylor expansion,

$$\Delta\Phi \approx \Lambda \Delta\varphi_r \quad (3.26)$$

with

$$\Delta\varphi_r = \frac{\partial\Phi}{\partial l_i} - \frac{\partial\Phi}{\partial l_j}. \quad (3.27)$$

This is the angle *accumulated* on the trajectory r (i.e. not reduced mod 2π). For the standard map, it is simply given by the sum of angular momentum values encountered on that trajectory,

$$\Delta\varphi_r = \tau \sum_{i=1}^n l_r(i) \quad l_r(1) = l_r(n) = l. \quad (3.28)$$

Thus, for a typical diffusive trajectory r ,

$$\langle \Delta\varphi_r \rangle = \tau \ln \quad (3.29)$$

and

$$\langle (\Delta\varphi_r - \langle \Delta\varphi_r \rangle)^2 \rangle = \tau^2 n \langle l^2 \rangle = \tau^2 n^2 D. \quad (3.30)$$

We can perform the sum (3.25) over the trajectories by first grouping those trajectories which lead to the same value of $\Delta\varphi$, and then summing over all values of $\Delta\varphi$. This will replace the sum over trajectories by a Fourier transform of the distribution of $\Delta\varphi$, whose mean and variance are given by (3.29) and (3.30). If it is assumed that this distribution depends on l only through (3.29), it follows that, upon averaging over l , the semiclassical approximation (3.25) vanishes for $\Lambda \neq 0$,

$$B(\Lambda; n) = 0 \quad \text{for } \Lambda \neq 0 \text{ and } n \lesssim n_{\text{qm}}. \quad (3.31)$$

The numerical data confirm this semiclassical result for $n \lesssim n_{\text{qm}}$, but only if $\Lambda \gg 1$. Semi-classical approximations of the present type are incapable, in principle, of describing the correlation function $B(\Lambda; n)$ for $n \gtrsim n_{\text{qm}}$, as the preceding discussion

shows. The study of this function for large times will therefore be based on numerical evidence alone.

In fact, a direct quantum mechanical calculation shows that $B(\Lambda; n)$ vanishes identically only for $n = 1$, but takes positive values, for sufficiently small Λ , already at $n = 2$.

Using the definition (3.3) of the amplitudes $A(l, n)$, we write $B(\Lambda; n)$ in the form

$$B(\Lambda; n) = \langle \langle l | U^n | l \rangle \langle l + \Lambda | (U^\dagger)^n | l + \Lambda \rangle \rangle \quad (3.32)$$

and substitute the Floquet operator for the QKR from (2.7).

For $n = 1$ we obtain, writing the average over l explicitly,

$$B(\Lambda; 1) = \lim_{L \rightarrow \infty} \frac{1}{2L+1} \sum_{l=-L}^L \exp(-\frac{1}{2}i\tau\Lambda(2l+\Lambda)) |J_0(k)|^2 \quad (3.33)$$

where $J_m(x)$ denotes ordinary Bessel functions. For $\Lambda \neq 0$ the sum over l vanishes in the limit $L \rightarrow \infty$, unless the condition $\tau\Lambda l = 2\pi m$ is fulfilled for some m . This is impossible for the generic case of irrational τ . Hence

$$B(\Lambda; 1) = |J_0(k)|^2 \delta_\Lambda. \quad (3.34)$$

For $n = 2$ we have

$$\begin{aligned} B(\Lambda; 2) &= \lim_{L \rightarrow \infty} \frac{1}{2L+1} \sum_{l=-L}^L \sum_{m, m'} \exp(i\tau l(2\Lambda + m - m')) \\ &\times \exp(\frac{1}{2}i\tau(2\Lambda(\Lambda - m') + m^2 - m'^2)) |J_m(k)|^2 |J_{m'}(k)|^2. \end{aligned} \quad (3.35)$$

Upon summation over l , only terms with $m' - m = 2\Lambda$ contribute and thus

$$B(\Lambda; 2) = \sum_m \cos(\tau\Lambda m) |J_{m-\Lambda}(k)|^2 |J_{m+\Lambda}(k)|^2. \quad (3.36)$$

An estimate of the Fourier sum in (3.36) is obtained if the Bessel functions are replaced by the crude approximation

$$|J_m(k)|^2 \approx \begin{cases} 1/2k & |m| \lesssim k \\ 0 & |m| \gtrsim k \end{cases} \quad (3.37)$$

which gives for $\tau \gg 1$

$$B(\Lambda; 2) \approx \begin{cases} \frac{1}{2k} \left(1 - \frac{\Lambda}{k}\right) & |\Lambda| \lesssim k \\ 0 & |\Lambda| \gtrsim k \end{cases} \quad (3.38)$$

i.e. $B(\Lambda; 2)$ is positive over a finite range of Λ .

This expectation is confirmed by the numerical data. Figure 8(a) shows two examples of the time dependence of $B(\Lambda; n)$ for different values of $\Lambda \neq 0$ but otherwise identical parameter values. $B(\Lambda; n)$ grows to finite values for $n > 1$ and approaches

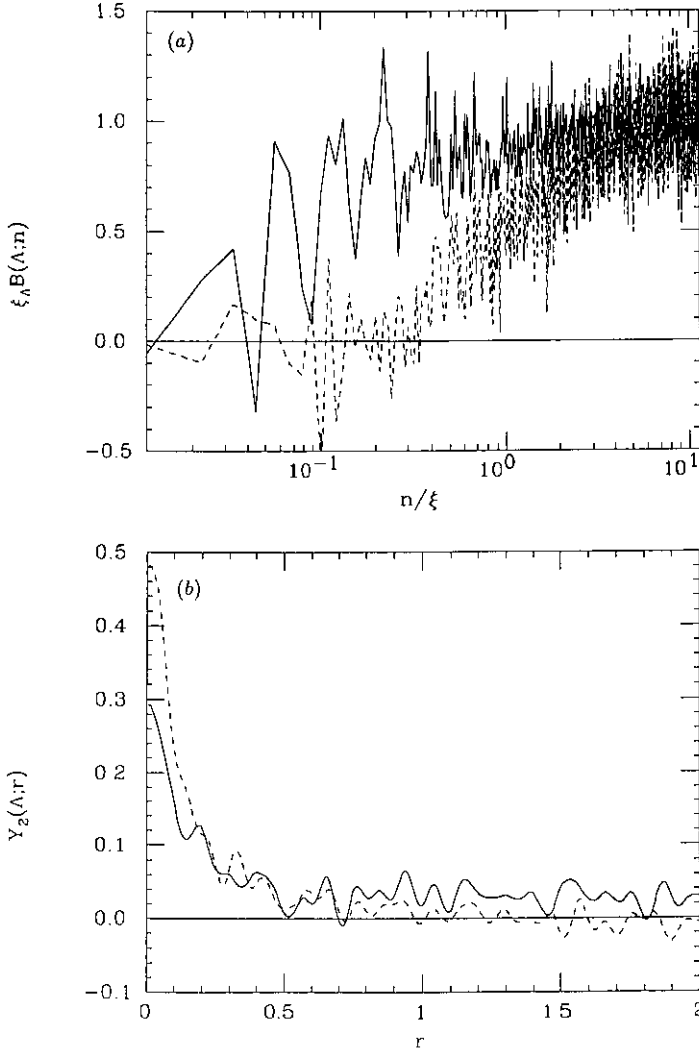


Figure 8. Scaled amplitude correlation function $B(\Lambda; n)/\gamma_\Lambda$ (a) and space-dependent cluster function $Y_2(\Lambda; r)$ (b) for the quantum kicked rotor. Parameter values are $K = 20$, $\tau = 0.1/((\sqrt{5} - 1)/2)$, and $\Lambda = 16$ (full lines), $\Lambda = 80$ (broken lines).

a positive asymptote for $n \rightarrow \infty$, but the onset occurs at increasingly later times as Λ increases. Applying the transformation (3.19), we obtain the corresponding examples of the space-dependent cluster function $Y_2(\Lambda; r)$, depicted in figure 8(b). The most important feature of these functions is that, for a fixed $\Lambda \neq 0$, they decay from a positive value at $r = 0$, indicating *negative* correlations (compare the discussion preceding (3.16)). This is in contrast to the behaviour of $Y_2^{\text{loc}}(r)$ ($= Y_2(0; r)$; see figure 6). The dependence on Λ of the long-time asymptote γ_Λ of $B(\Lambda; n)$ is shown in figure 9(a). For sufficiently large Λ , γ_Λ decays exponentially, as should be expected from (3.20), given exponential localization of the Floquet eigenstates. For small Λ an additional structure appears; the decay from $\gamma_0 = \xi^{-1}$ to γ_1 , in particular, is abrupt. A corresponding singularity is observed in the dependence of $Y_2(\Lambda; 0)$ on Λ (figure 9(b)).

It shows that the switching from positive correlations at $\Lambda = 0$ to negative correlations for $\Lambda \neq 0$ occurs immediately between $\Lambda = 0$ and 1. $Y_2(\Lambda; 0)$ remains approximately constant for $\Lambda \lesssim \xi$ and then decays to zero, reflecting the absence of correlations between sufficiently separated localization neighbourhoods.

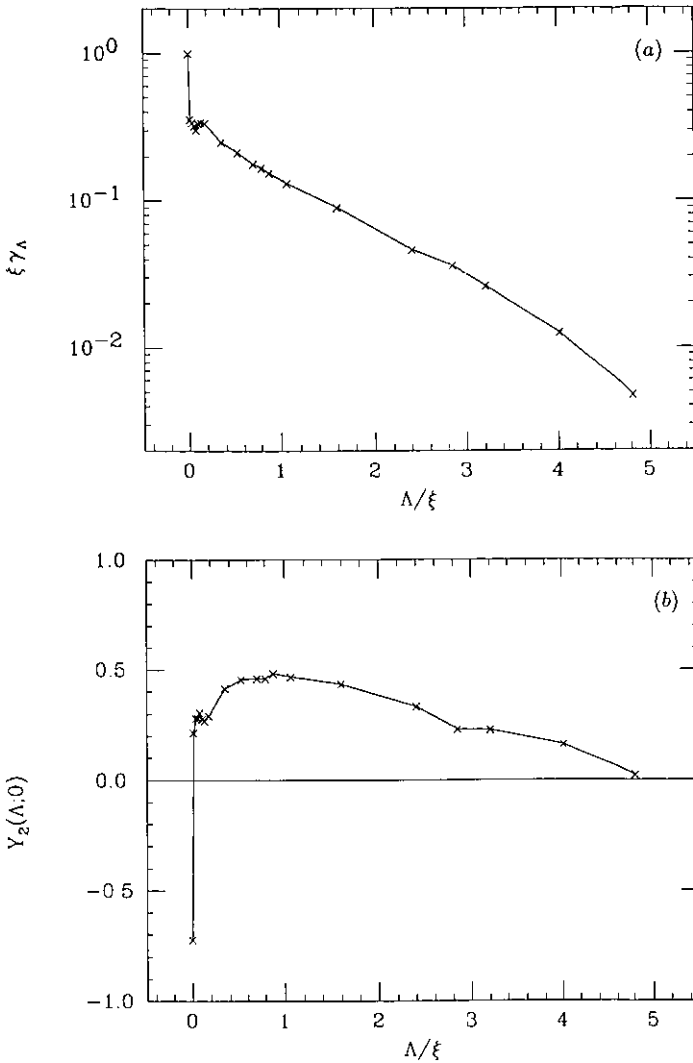


Figure 9. Generalized inverse participation ratio γ_Λ (a) and space-dependent cluster function $Y_2(\Lambda; r)$ at $r = 0$ (b), as functions of the scaled parameter Λ/ξ , for the quantum kicked rotor. Parameter values are $K = 20$ and $\tau = 0.1/((\sqrt{5} - 1)/2)$. Lines connecting the data points serve to guide the eye.

The asymptotic equivalence (3.22), for large times n , of the transition probabilities $P_l(\Lambda; n)$ and the space-dependent amplitude correlator $B(\Lambda; n)$ can be used to obtain results for the long-time asymptotes γ_Λ , independently from the data shown in figure 9(a). Figure 10 shows the values $\lim_{N \rightarrow \infty} (1/N) \sum_{n=0}^{N-1} P_l(\Lambda; n)$ as a function of Λ , i.e. the *average* 'stationary state' of the QKR, if only a single l state is initially excited (note that the parameter values here are different from those used in figure 9(a),

but agree in the value $k = 19.67$). Since the calculation of these data is numerically less costly than the determination of the γ_Λ according to (3.12), a denser set of data points than in figure 9 could be obtained. The exponential decay of γ_Λ for large $|\Lambda|$ coincides with the result shown in figure 9(a); the apparent interference pattern around the central peak at $\Lambda = 0$ can be seen in much more detail (cf the inset in figure 10). While, phenomenologically, this interference pattern closely resembles a Bessel function dependence $\sim |J_\Lambda(k)|^2$, we still lack a theoretical explanation for it.

It is particularly instructive to compare these numerical findings with analytical results for the space-dependent level correlation function in one-dimensional systems with Anderson localization, reported in [11] (figure 1 in that reference provides a summary of those results and corresponds to our figure 9(b)—note that in [11], the correlation function $P_2(\Lambda; 0)$ is depicted and not $Y_2(\Lambda; 0)$, with correspondingly different sign conventions). The qualitative agreement is striking. It should be emphasized that, in the case of a *one-dimensional* disordered solid as discussed in [11], the repulsion of the bare levels is exactly compensated by the Mott mechanism explained above, while only in the *two- and higher-dimensional* solid state analogue are there positive correlations in the local spectrum at $\Lambda = 0$ [12]. The agreement clearly demonstrates that the features we observe in $Y_2(\Lambda; r)$ are indeed a direct consequence of localization and should be explained in terms of quantum mechanical interference. Therefore, a semiclassical description of these phenomena cannot be achieved as long as dynamical localization, in general, is not understood on the semiclassical level.

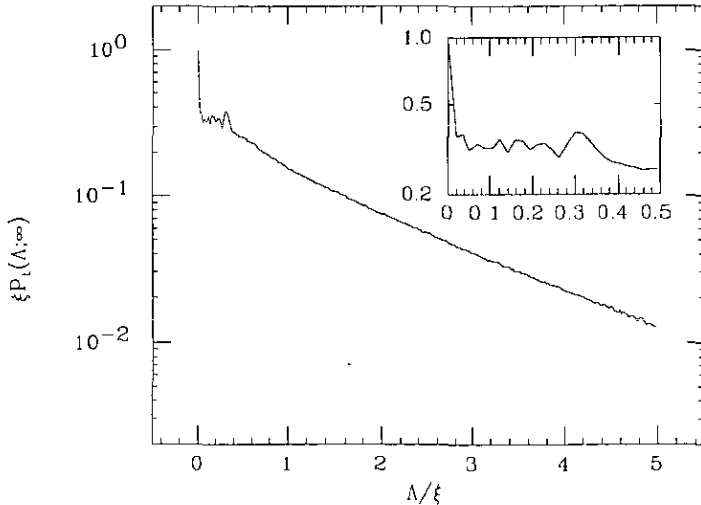


Figure 10. Asymptotic transition probability $P_1(\Lambda; \infty)$ for the quantum kicked rotor, as a function of the scaled parameter Λ/ξ . Parameter values are $K = 10$ and $\tau = 0.05/((\sqrt{5} - 1)/2)$. The inset shows the enlarged section $0 \leq \Lambda/\xi \leq 0.5$ of the same function.

4. Measuring spectral two-point correlation functions

The results obtained in section 3 emphasize the significance of the spectral two-point correlation function as a source of information on basic dynamical properties.

It appears desirable, therefore, to establish a 'correlation spectroscopy' also on the experimental level.

Spectral two-point correlation functions in periodically driven systems are analogous to the *ac* conductivity, which plays a similar role to a basic physical characteristic in solid state theory. This analogy suggests a simple experimental access to spectral correlations: it consists in probing the system by means of a small periodic perturbation, with a frequency ϵ on the scale of typical QE separations. The probabilities of transitions between Floquet states, induced by the perturbation, represent measurable quantities which provide information on two-point correlations in the QE spectrum.

Specifically, assume a perturbation of the form

$$W(t) = W \sin(\epsilon t) \sum_{n=-N/2}^{N/2} \delta(t - n\tau) \quad (4.1)$$

lasting over a time span $-N\tau/2 \leq t \leq N\tau/2$ (for formal convenience, we choose a perturbation pulsed in the same way as the potential in a kicked system). Time-dependent perturbation theory then yields the transition amplitudes

$$A_{\alpha \rightarrow \beta} = \frac{2\pi}{N} \langle \alpha | W | \beta \rangle (\delta_N(\omega_\alpha - \omega_\beta - \epsilon) - \delta_N(\omega_\alpha - \omega_\beta + \epsilon)). \quad (4.2)$$

The finite time span $N\tau$ during which the system is probed allows only for a limited frequency resolution. This is expressed in the occurrence of broadened pulses of the form

$$\delta_N(x) = \frac{1}{2\pi} \sum_{n=-N/2}^{N/2} e^{inx} \quad (4.3)$$

with a width π/N and a maximum value $N/2\pi$, in (4.2). Accordingly, the probability of finding the initial QE distribution $P_i(\omega_\alpha)$ altered at some QE ω_β , is given by the convolution

$$\begin{aligned} P_\epsilon(\omega_\beta) &= \sum_{\substack{\alpha \\ \alpha \neq \beta}} P_i(\omega_\alpha) |A_{\alpha \rightarrow \beta}|^2 \\ &= N^2 \sum_{\substack{\alpha \\ \alpha \neq \beta}} |\langle \alpha | W | \beta \rangle|^2 (\Delta_N(\omega_\alpha - \omega_\beta - \epsilon) + (\Delta_N(\omega_\alpha - \omega_\beta + \epsilon))) \end{aligned} \quad (4.4)$$

where Δ_N is another type of broadened pulse, with a width π/N and a normalized maximum value 1 (interferences between the positive and the negative pulse in (4.2) can be neglected if N is sufficiently large).

The occurrence of the weights $|\langle \alpha | W | \beta \rangle|^2$ in (4.4) provides the possibility of determining various types of QE correlations by tailoring the perturbation operator W appropriately. In particular, if W is chosen as a 2^Λ -pole operator, i.e.

$$W = w \sum_l (|l\rangle \langle l + \Lambda| + |l + \Lambda\rangle \langle l|) \quad (4.5)$$

(4.4) becomes

$$P_\epsilon(\omega_\beta) = N^2 w^2 \sum_{\substack{\alpha \\ \alpha \neq \beta}} P_i(\omega_\alpha) (\Delta_N(\omega_\alpha - \omega_\beta - \epsilon) + \Delta_N(\omega_\alpha - \omega_\beta + \epsilon)) \sum_l |\langle \alpha | l \rangle|^2 |\langle \beta | l + \Lambda \rangle|^2 \quad (4.6)$$

corresponding to a measurement of the *local* two-point correlation function with the spatial argument Λ (see section 3). If, on the other hand, W is chosen very broad in the basis of kinetic energy eigenstates, $P_\epsilon(\omega_\beta)$ conveys information on the *unbiased* QE spectrum.

The idea expounded in this section finds its most natural practical application in the experimental study of the QE spectrum of Rydberg atoms driven by microwave fields. There, a second driving field with variable frequency is used as a probe to measure changes in the excitation pattern. A detailed analysis of this procedure was recently given in [29], and preliminary experimental results are reported in [30].

5. Summary

In the present work we investigate the quasi-energy spectrum of the kicked rotor in order to identify the fingerprints of dynamical localization in the spectral statistics. A systematic approach to incorporate the specific spatial structure represented by localized Floquet eigenstates in the definitions of spectral correlation functions is provided by the *local spectrum*: it is conceptually different from the common spectrum in that the contribution of each QE is endowed with an individual weight, equal to the overlap of the corresponding eigenstate with a reference state in the unperturbed basis.

The *local spectrum* of the QKR is characterized by positive correlations on small QE scales, corresponding to an apparent attraction of levels. Since the local two-point correlation function is the Fourier transform of the mean probability to stay at the initial state, positive correlations reflect the crossover from a diffusive decay of the staying probability to quasi-periodic behaviour in the long-time limit. Level clustering in the local spectrum is not, as it may seem, at variance with the known view that this crossover comes about by the resolution of ever finer QE scales with increasing time: at avoided crossings, which dominate the small QE scales, quasi-energies are associated with eigenstates showing two (or more) centres of localization. Such ‘double-hump states’ endow quasi-energies at avoided crossings with a sufficiently high weight in the local spectrum such that level repulsion in the unbiased spectrum is effectively masked.

An important feature, which has not been noticed until now in the context of dynamical localization, is the discontinuity in the spectral-spatial correlations at $\Lambda = 0$ (figure 9(a,b)). This phenomenon is due to the fast fluctuations of the phases of the amplitudes $\langle l | \alpha \rangle$ on a scale $\Delta l = 1$, which occur together with the mean smooth decay of $|\langle l | \alpha \rangle|^2$ on the scale of the localization length. This phenomenon is a necessary consequence of the localization mechanism. Its presence is well established in Anderson localized states, where it induces phenomena similar to those observed in the present context.

A possibility to measure two-point correlation functions of local spectra in a system with dynamical localization, and thus an experimental test of our theory, is provided by slightly extending the set-up for the microwave excitation of Rydberg atoms: the change in the excitation pattern caused by a second driving field with variable frequency can serve as a probe of spectral correlations.

Acknowledgments

We have profited from discussions with R Graham, J L Pichard, J Imry, F Izrailev and B Al'tshuler. M V Berry made very useful comments on the manuscript. We are most obliged for their help. TD would like to thank the Department of Nuclear Physics at the Weizmann Institute in Rehovot for the warm hospitality extended to him during a postdoctoral stay and acknowledges financial support by *Minerva*. Part of this work was carried out while US was a visitor at the Institut de Physique Nucléaire in Orsay. He would like to thank Dr O Bohigas for his hospitality and for stimulating discussions.

References

- [1] Zaslavsky G M 1979 *Usp. Fiz. Nauk* **129** 211 (Engl. transl. 1979 *Sov. Phys.-Usp.* **22** 788)
Bohigas O and Giannoni M J 1984 *Chaotic Motion and Random Matrix Theories (Lecture Notes in Physics 209)* (Berlin: Springer) p 1
Berry M V 1985 *Proc. R. Soc. A* **400** 229
- [2] Blümel R and Smilansky U 1988 *Phys. Rev. Lett.* **60** 477; 1989 *Physica D* **36** 111
- [3] Fishman S, Grempel D R and Prange R E 1982 *Phys. Rev. Lett.* **49** 509; 1984 *Phys. Rev. A* **29** 1639
- [4] Shepelyansky D L 1986 *Phys. Rev. Lett.* **56** 677
- [5] Dyson F J 1962 *J. Math. Phys.* **3** 140, 1191
- [6] Porter C E 1965 *Statistical Theory of Spectral Fluctuations* (New York: Academic)
- [7] Feingold M, Fishman S, Grempel D R and Prange R E 1985 *Phys. Rev. B* **31** 6852
- [8] Molcanov S A 1981 *Commun. Math. Phys.* **78** 429
- [9] Izrailev F M 1986 *Phys. Rev. Lett.* **56** 541
- [10] Heller E J 1987 *Phys. Rev. A* **35** 1360
- [11] Gor'kov L P, Dorokhov O N and Prigara F V 1983 *Zh. Eksp. Teor. Fiz.* **84** 1440 (Engl. transl. 1983 *Sov. Phys.-JETP* **57** 838)
- [12] Sivan U and Imry Y 1987 *Phys. Rev. B* **35** 6074
- [13] Al'tshuler B L and Shklovskii B I 1986 *Zh. Eksp. Teor. Fiz.* **91** 220 (Engl. transl. 1986 *Sov. Phys.-JETP* **64** 127 (1986))
- [14] Mott N F 1970 *Phil. Mag.* **22** 7
- [15] Dittrich T and Smilansky U 1991 *Nonlinearity* **4** 85–101
- [16] Frahm H and Mikeska H J 1988 *Phys. Rev. Lett.* **60** 3
- [17] Feingold M, Fishman S, Grempel D R and Prange R E 1988 *Phys. Rev. Lett.* **61** 377
Frahm H and Mikeska H J 1988 *Phys. Rev. Lett.* **61** 378 (Reply)
- [18] Blümel R, Goldberg J and Smilansky U 1988 *Z. Phys. D* **9** 95
- [19] Izrailev F M 1988 *Phys. Lett.* **134A** 13; 1989 *J. Phys. A: Math. Gen.* **22** 865
- [20] Chirikov B V 1979 *Phys. Rep.* **52** 263
- [21] Casati G, Chirikov B V, Izrailev F M and Ford J 1979 *Lecture Notes in Physics* vol 93 (Berlin: Springer) p 334
- [22] Enß V and Veselić K 1983 *Ann. Inst. Henri Poincaré A* **39** 159
- [23] Izrailev F M and Shepelyansky D L 1979 *Dokl. Akad. Nauk* **249** 1103 (Engl. transl. 1979 *Sov. Phys.-Dokl.* **24** 996); 1980 *Teor. Mat. Fiz.* **43** 417 (Engl. transl. 1980 *Theor. Math. Phys.* **43** 553)
- [24] Casati G and Guarneri I 1984 *Commun. Math. Phys.* **95** 121
- [25] Casati G, Ford J, Guarneri I and Vivaldi F 1986 *Phys. Rev. A* **34** 1413
- [26] Guarneri I 1989 *it Europhys. Lett.* **10** 95
- [27] Chirikov B V, Izrailev F M and Shepelyansky D L 1981 *Sov. Sci. Rev. C* **2** 209
- [28] Blümel R, Fishman S and Smilansky U 1986 *J. Chem. Phys.* **84** 2604
- [29] Blümel R and Smilansky U 1990 *Theory of High Order Processes in Atoms in Intense Laser Fields* ed K Kulander and A l'Huillier *J. Opt. Soc. Am. B* feature issue in press
- [30] Buchleitner A 1989 *Diploma Thesis* LMU München, unpublished